Microchemical Journal 177 (2022) 107219

Contents lists available at ScienceDirect

Microchemical Journal

journal homepage: www.elsevier.com/locate/microc

An innovative electron paramagnetic resonance and statistical analysis approach to investigate the geographical origin of multi-layered samples from a Renaissance painting

Maurizio Romanelli [a,1], Antonella Buccianti [a], Francesco Di Benedetto [b,*], Lorenzo Bellucci [c], Stefan Cemicky [c]

[a] Dipartimento di Scienze della Terra, Università degli Studi di Firenze, via G. La Pira, 4, 50121 Firenze, Italy
[b] Dipartimento di Fisica e Scienze della Terra, Università degli Studi di Ferrara, Via G. Saragat, 1, 44121 Ferrara, Italy
[c] DRIART AG – Embraport 1, 8424 Embrach, Zurich, Switzerland

ARTICLE INFO

Keywords:
Renaissance painting
EPR spectroscopy
Statistical analysis
Provenance
Calcite

ABSTRACT

The present study aims at unravelling whether an innovative, integrated method based on electron paramagnetic resonance (EPR) spectroscopy and statistical analysis could shed light on the mineralogical attribution of calcium carbonate, $CaCO_3$, microcrystalline powders found in an unusual preparation layer of a Renaissance painting on wood. Moreover, the undertaken investigation was performed to assess, if possible, the geographical provenance of the same carbonate powders. A specifically designed procedure was operated based on previous methods applied to the investigation of ancient white and colored marbles.

Microscopic samples were taken from the painting with the aim of keeping both their size and mass at a minimum possible. All investigated samples consist of a highly complex, multi-layered, heterogeneous material, where the calcium carbonate aliquot is very limited. The investigation has been carried out in a non-destructive way, registering the EPR spectra of the fragments, identifying the diagnostic Mn(II) spectra, parameterizing them, and comparing them with the most extensive available database through a set of robust statistical methods. The main results include the attribution to calcite (marble rather than chalk), the mineralogical speciation of the carbonate layer and the reduction of the possible calcite provenance sites to few localities where marble was exploited. Among them, the marble from Apuan Alps is one of the likely provenances of this calcite.

1. Introduction

Determining the provenance of materials used in the realization of an artwork is a matter of great interest, linked to the reconstruction of the social and economic context in which the author accessed the materials and operated on them. The materials could have been available either at local or at a regional scale, therefore easily achievable by the artist, or pertaining to remote sources, and thus available by trade routes only. Accessing this information is, in general, a challenging task. For minerals and rocks, used as building materials, in sculpture, in pigments, etc., this task can be accomplished by tracing specific fingerprints (chemistry, structure, isotope composition, phase composition, texture, etc.) by which one can relate experimental findings in the materials contained in a specific artwork to those observed in a supposed (or documented) mineralization.

In the last couple of decades, the application of the electron paramagnetic resonance spectroscopy method and the exploration of its capabilities for tracing the provenance of ancient and Renaissance white marbles received significant attention. This procedure, initially proposed by Armiento et al. [3–4], Attanasio [5], and Baïetto et al. [13], was exploited and refined, finding application in several relevant, sometimes world-renowned, case studies (e.g., [1,7,12,8,16,17,27,36]). To date, all the successful applications of this procedure pertain to the investigation of statuary materials. To the best of the authors' knowledge, no attempts to pursue a similar approach in determining calcite-bearing materials in paintings are found in the literature. Accordingly, in this study, we want to explore the adaptation of Attanasio's [5] method and its feasibility in the determination of the provenance of

* Corresponding author.
E-mail address: francesco.dibenedetto@unife.it (F. Di Benedetto).
[1] Now retired.

https://doi.org/10.1016/j.microc.2022.107219
Received 23 November 2021; Received in revised form 15 January 2022; Accepted 16 January 2022
Available online 20 January 2022

$CaCO_3$ microcrystalline powders contained in a painting.

The case study is given by a painting belonging to a private collection representing the "Last Judgment," subject of the world-famous Michelangelo Buonarroti's fresco in the Sistine Chapel (Rome, Vatican City). This artwork, belonging to the Renaissance period [28], was the object of a recent in-depth systematic multi-methodical investigation. During this investigation, a very smooth, powdery, and homogeneous $CaCO_3$ ground preparation layer, covering the entire wooden support and underlying both drawing and painting layers, was revealed by microsampling. The present study is specifically aimed at investigating the nature of the unexpected calcium carbonate phase. Specifically, two questions can be raised:

1. Which kind of $CaCO_3$ polymorph (calcite, aragonite, or both) constitutes the preparation layer?
2. Is it possible to determine the geographical origin of such carbonate material?

The answer to the above questions is provided by an innovative method that adapts the already available procedures described in the literature to this specific case. The study combines both EPR spectroscopy and robust statistical analysis of the spectroscopic findings.

The study consists of: a revision of the main principles of the provenance studies based on the EPR technique (Section 2); the experimental strategy and procedures (Section 3); the spectroscopic results and the statistical analysis of the affinity of the present results with groups in the Attanasio's [6] database (Section 4). Finally, in Section 5, the above critical questions of the study are addressed.

2. The EPR spectrum of Mn(II) in $CaCO_3$ for provenance studies

The X-band EPR spectrum of Mn(II) in $CaCO_3$ is determined by the interactions affecting the spin system, i.e. the prevailing Zeeman interaction [15,32] and hyperfine and fine interactions. From a spectroscopic point of view, its most informative part consists in six lines due 'allowed' transitions and in ten weaker lines due to 'forbidden' transitions. The line width is narrow enough [14] to consider a number of additional and significant details experimentally detectable, in particular those concerning the Crystal Field surrounding the Mn(II) ion [15,32].

The diagnostic applications of the spectrum were already presented decades ago. The information derived from the interpretation of the spectral parameters allowed to trace phenomena linked to the replacement of Ca with other ions [40,2] or to unravel inhomogeneity of the short range distribution of Mn and Mg in replacing Ca [38,26]. Indeed, a further feature to which most of the spectral variability can be attributed is provided by the occurrence of the variable distribution of the fine interaction [39], which causes the spectrum to exhibit subtle but appreciable changes in the experimental line width. This effect is mostly detected in the high field lines of the hyperfine sextet. These spectroscopic features arise from specific crystal-chemical occurrences in the mineral. In principle, Mn(II) replaces Ca in the distorted octahedral site of calcite. The distortion of the polyhedron, -3 site symmetry, causes the anisotropy of the hyperfine and fine interactions. Studies carried out on double carbonates, e.g., dolomite $CaMg(CO_3)_2$, revealed that Mn can replace both Ca and Mg, giving rise to different spectral contributions superimposable in the experimental EPR spectrum. The strength and anisotropy of the fine interaction are more significant in the case of Mn replacing Mg due to the smaller site volume of this latter ion.

In calcite, Ca can be replaced by both Mn and other ions, e.g., Fe(II), Co(II), Sr, and Mg (in small amounts). A long-range order of impurities in the calcite lattice cannot be attained. In such a case, Mn could replace Ca in a site where all the first cationic neighbors are still Ca ions or in further sites where the Ca neighboring ions are variably replaced by other impurities. Accordingly, several different spectral possibilities arise, giving rise to a distribution of the fine interaction. In the literature, it is namely the distribution of the fine interaction that has been attributed of the major role in "tracing" marble and other carbonate samples through EPR (e.g., [32,39]).

The specific applications of the EPR spectroscopy in the field of cultural heritage and archaeometry firstly provided by Attanasio [5], suggest that the interpretation of the EPR spectrum of Mn(II) in calcite can convey information on the provenance of ancient white marbles used in the classical and renaissance sculpture. The study proceeds by comparing spectra of marble samples collected in the historical quarries likely used for the marble apportionment. The comparison was validated using multivariate statistical techniques, driven through a phenomenological parameterization of the experimental spectrum. The method was highly successful, and in the last two decades, several statues of different epochs and localities were characterized [1,7,12,8,16,17,27,36]. Successful applications were also operated on colored marbles (e.g., [11,17,41]). The method was then improved, including other parameters in the database, as, eminently, carbon and oxygen isotope ratios, and the mean particle size, determined by optical microscopy [9,10].

One must mention that other approaches, based on similar assumptions have been described in the literature [18,19,23,22,29,39,30,21]. In particular, Duliu and Velter-Stefanescu [22] proposed a method based on the parameterization of the first hyperfine line (the original method proposed by [5], is mainly based on details of the sixth line), coupled with cluster analysis. Piligkos et al. [29] and Weihe et al. [39] proposed a robust parameterization obtained by the exact determination of all the contributions to the spin Hamiltonian, including the distribution of the fine interaction obtained by numerical simulation. A similar approach was also pursued by Di Benedetto et al. [21], where a parameterization by spectral simulation, coupled with robust statistical methods derived from the compositional data analysis (CoDA), turned out highly efficient in discriminating carbonate rocks.

3. Experimental procedures

3.1. The artwork

The studied artwork is an oil painting on wood (Fig. 1), belonging to a private collection, and representing the "Last Judgment", subject of the world-famous Michelangelo Buonarroti's fresco in the Sistine Chapel (Rome, Vatican City). The wood support consists of two elements of 129.5×100 cm^2 and 128.5×15 cm^2, respectively, assembled to form a trapezoidal panel of overall dimensions B = 129.5 cm, b = 128.5 cm, h = 115 cm.

In 2006, a robust systematic scientific investigation campaign on the painting was initialized. An integrated multi-methodical approach based on historical, stylistic, and forensic investigations was applied. This study aimed to assess authorship, origin, history, conservation issues, execution details, and materials used in the painting, and it will be the object of a forthcoming publication.

Among applied analytical methods, microscopic samples were extracted and analyzed by both light and SEM microscopy, combined with spectroscopic analytics. The sample stratigraphy provided a significant but also puzzling clue. The preparation layer, applied onto the wood to create a homogenous, whitish layer for sketching and painting, consists of $CaCO_3$ (Fig. 2), while it is generally accepted that Italian masterpieces of the first half of the 16th-century contain preparation layers made up of gypsum, $CaSO_4{\cdot}2H_2O$, mixed with animal glue as a binder [35]. On the contrary, Northern European painters usually applied a calcite preparation layer on their painting's supports, and this phase was supplied by chalk quarries [34]. Therefore, the identification of $CaCO_3$ in the preparation of an early 16th century painting usually suggests a region north of the Alps as the geographical origin of the artwork. In this case, however, the preliminary morphological investigation of the sampled aliquots revealed a very homogenous, powdery granulometry (1–3 μm particles) in the calcite layer, as well as the absence of any other materials (Fig. 2 a-d). This unique appearance strongly differs from the usual morphology of the 16th-century chalk-

Fig. 1. The Renaissance painting object of the study (modified from [28]).

based preparation layers from Northern Europe. As a consequence, the exact identification of $CaCO_3$ and its geographical origin became crucial to address the matter.

3.2. Sampling procedures

Eleven fragments were extracted from the painting under a stereomicroscope with the aid of a micro-scalpel. All samples, sub-millimetric in size and weighting a few mg, have a truncated triangular prism section. The main surface is the one containing the pictorial layers. All samples exhibit a heterogeneous layered phase composition (Fig. 2), including all layers from the preparation up to the outer surface. Indeed, the $CaCO_3$ layer represents a very small aliquot of the total sample mass. $CaCO_3$ in the considered samples was revealed in the preparation layer only.

3.3. Strategy of the EPR investigations

The application of the procedures described in the literature [5,7,19,22,39,30,21] to a painted wood panel, object of the present study, is not straightforward. The samples available for the current study are extracted from a composite, multi-layered material, where $CaCO_3$ is only contained in a single internal layer, so that the amount of material is severely limited. $CaCO_3$ cannot be physically separated from nor the wood nor the overlying layers.

We decided to follow a procedure roughly similar to that proposed by

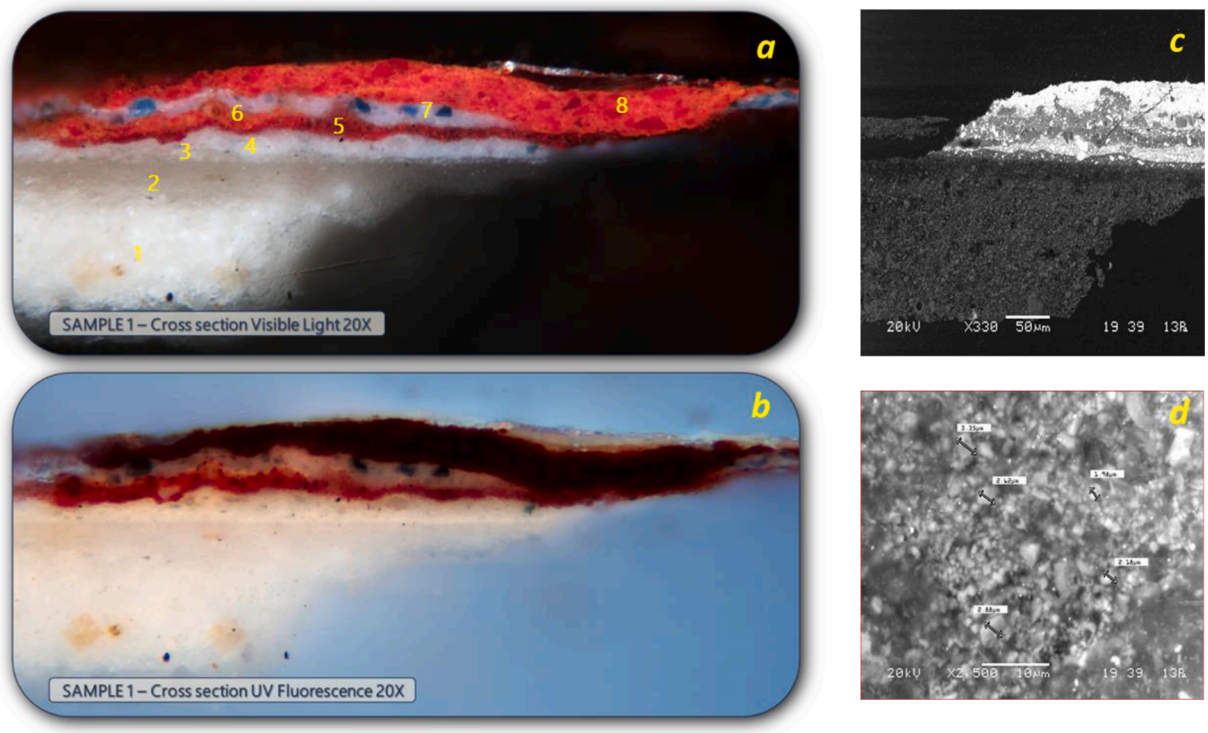

Fig. 2. Cross-section, observed at optical (a, b) and electronic (c, d) microscopes. Optical cross-section micrographs were obtained under Visible (a) and UV (b) light. The eight different layers are: $CaCO_3$ preparation layer (1); animal glue layer (2); lead white priming (3); lead white, and azurite pictorial layer (4); red varnish (5); cinnabar pictorial layer (6); lead white, and azurite pictorial layer (7); cinnabar final pictorial layer (8).

Attanasio [5–6]. Concerning the other studies cited in the 2.1 paragraph, we want here to emphasize the main constraints/limitations we were forced to face:

1. the necessity of comparison with an already established database for studying the material provenance. Attanasio [6,10] presented the most significant number of sites, covering most of the quarries of white marbles in the Mediterranean basin.
2. the impossibility to perform isotopic investigations on the samples, although these parameters were part of Attanasio's (2006) database.
3. the impossibility to attain reliable quantitative parameters from the absolute intensity in the EPR spectra, on which Attanasio's [6] procedure was based.

Accordingly, we identified only three parameters of the EPR spectra as reliable under the limits of the present study. These data were then compared with the database reported in Attanasio [6], limited to such parameters only. These parameters are defined in the next paragraph.

3.4. EPR spectral parameters

An exemplar EPR spectrum of one of the investigated samples, exhibiting the signal of Mn(II) in calcite in the selected field region, is shown in Fig. 3a. The spectrum was parameterized, according to the indications provided by Attanasio [5–6], employing five relevant field positions, corresponding to the positive peak of the first line of the Mn (II) sextet (position "I" in Fig. 3b), and to the positive and negative peaks of the sixth line of the same sextet (positions "II" to "V" in Fig. 3c). The uncertainty in measuring the field values is limited by the experimental field step, 0.039 mT, which is indeed assumed as an uncertainty value. From the magnetic field positions "I" to "V", three independent spectral parameters defined by Attanasio [6] can be determined from the following relations:

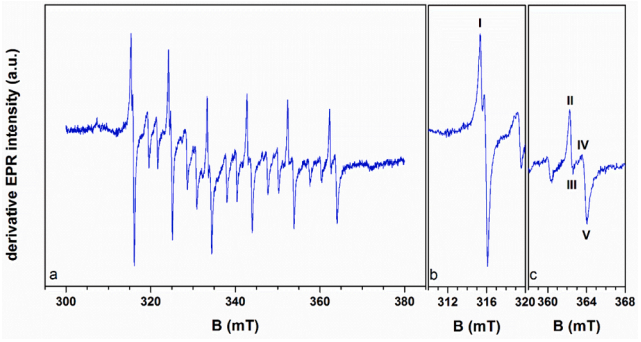

Fig. 3. a) Exemplar experimental EPR spectrum of the "2" investigated sample. Details of the first, b), and of the sixth, c) line of the Mn(II) sextet, with indications of the five relevant positions for the parameterization of the spectrum.

$$SPREAD = B_V - B_I \tag{1}$$

$$SPLI = \frac{B_V + B_{IV}}{2} - \frac{B_{II} + B_{III}}{2} \tag{2}$$

$$WAV = \frac{(B_{III} - B_{II}) + (B_V - B_{IV})}{2} \tag{3}$$

The first parameter, SPREAD, is mainly related to the hyperfine interaction, the second parameter, SPLI, refers to the average fine interaction, whereas the third, WAV, refers to both the line width and the distribution of fine interaction. The uncertainties in the derived SPREAD, SPLI, WAV values were obtained by propagating the experimental uncertainties in the field position and intensity.

3.5. Experimental EPR procedures

The samples were analyzed without any pre-treatment or manipulation by simply inserting them in amorphous silica tubes. These tubes were chosen to avoid the presence, in the glassy matrix, of transition metal impurities, which would likely interfere with the EPR spectra of the samples. Since no EPR spectra were present in the literature (to the best of the authors' knowledge), a chalk sample from Meudon (Paris, France) was also provided. In this case, the sample was prepared for the investigation by putting an aliquot of microcrystalline chalk powders, without any kind of pre-manipulation, in a Teflon bag. This, in turn, was placed inside the amorphous silica tubes.

The EPR spectral measurements were carried out using a conventional Bruker ER 200D-SRC, operating at ~9.5 GHz (X-band). Spectra were registered according to the following conditions: 0.5 mT modulation amplitude, 100 kHz modulation frequency. The post-amplification gain setup was optimized, sample by sample, to maximize the signal-to-noise ratio. Frequency was calibrated through the reference signal of the DPPH (1,1-Diphenyl-2-Pycrylhydrazyl) radical, used as an external standard. All spectra were registered in the 300–380 mT magnetic field range, with a field step of 0.039 mT and at a scan speed of 0.2 mT/s.

4. Results

The EPR investigations carried out on the 11 fragments of the painting provided evidence of the ubiquitous presence of Mn in the $CaCO_3$ layer. The exemplar spectrum presented in Fig. 3a can be easily compared with those shown in the comprehensive literature on EPR spectroscopy of Mn-bearing calcite, supporting the attribution of Mn to the Ca site in calcite [5,7,19,22,39,30,21,40,2,38,20,26,15,32,14]. This finding thus allows us to safely confirm that the carbonate preparation layer of the artwork consists of calcite.

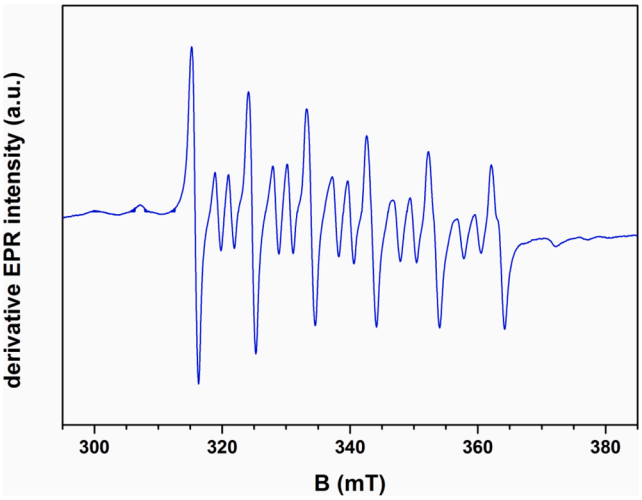

Fig. 4. Experimental EPR spectrum of the investigated sample of chalk.

The EPR spectrum of the chalk sample is shown in Fig. 4. Apparently, a pattern like the one illustrated in Fig. 3a can be noticed. However, the fine details are markedly different. Namely, the typical line indentations and/or splitting of the Mn(II) calcite patterns [39,21] are entirely missing in this spectrum. Conversely, the worse spectral resolution observed in the chalk EPR spectrum can be attributed to chemical disorder, poor crystallinity in the sample, or both. The close comparison of the whole EPR spectrum of the chalk sample (Fig. 4) with those of the specimens from the painting (Fig. 3a) safely allows excluding that the calcite layer consists of chalk.

The intensity of the spectrum, intended as a signal-to-noise ratio (Fig. 3a), and its intrinsic line width were good enough to allow a meaningful parametrization, according to the criteria described in §3.4, for 8, out of the 11 samples (spectra are illustrated in the Supplementary Materials file). For the other 3 spectra, the very poor signal-to-noise ratio prevented further parameterization. Remarkably, no experimental spectra' smoothing, nor noise reduction were operated, to avoid possible spurious correlations, especially with the WAV parameter. Both the list of the spectral parameters and the list of the values for the 3 derived parameters are presented in Table 1.

5. Discussion

The statistical analysis of spectrometric data was performed to highlight the similarity of the samples, extracted from the artwork with respect to the raw material collected in the different excavation sites contained in the database. The samples associated with the piece are n = 8 while the rest of the database consists of 1061 cases discriminated in 14 groups (Afyon, n = 65; Altıntaş, n = 58; Aphrodisias, n = 60; Carrara, n = 146; Denizli, n = 41; Ephesus, n = 50; Hymettus, n = 42; Miletus, n = 60; Naxos, n = 40; Paros, n = 142; Pentelic, n = 78; Proconnesus, n = 158; Thasos, n = 69; Thiounta, n = 44). The spectrometric data considered in the analysis were given by SPLI, SPREAD and WAV.

In Fig. 5a, b, and c, the violin plots allow us to visualize the comparison between the parameters of the artwork (group 15) with that of the different groups for SPLI, SPREAD, and WAV, respectively. A violin plot plays a similar role as a boxplot. It shows the distribution of quantitative data across several levels of one (or more) categorical variables so that those distributions can be compared. Unlike a boxplot, where all the plot components correspond to actual data points, the violin plot features a kernel density estimation of the underlying distribution. This can be an effective and attractive way to show multiple distributions of data at once. Still, one should keep in mind that the sample size influences the estimation procedure, and violins for relatively small samples might look misleadingly smooth [24,37]. As we can see, there is a lot of overlapping for WAV and SPREAD for all the groups while SPLIT shows a clear separation among the piece and the other groups and some similarity with group 4 (Carrara), characterized by a clear shift toward low values for all the data body. It is important to stress that the material sampled around the Mediterranean basin is related to the original rock. In contrast, the samples extracted from the painting could have suffered the effect of different sample preparation

Table 1
List of the experimental values of the EPR parameters determined in this study. All values are expressed in Gauss to conform to the format of the Attanasio [6] database. 1 Gauss = 0.1 mT.

Sample	I	II	III	IV	V	SPREAD	SPLI	WAV
S1	3153.49	3622.05	3626.52	3634.32	3641.29	487.80	13.52	5.72
S2	3153.46	3622.74	3625.71	3636.24	3640.58	487.12	14.19	3.66
S3	3152.14	3620.81	3624.40	3634.90	3639.73	487.59	14.71	4.21
S4	3153.6	3622.76	3625.52	3636.02	3640.89	487.29	14.32	3.82
S5	3153.98	3622.9	3625.96	3637.20	3640.97	486.99	14.66	3.42
S6	3152.71	3622.74	3625.76	3636.56	3641.26	488.55	14.66	3.86
S7	3153.87	3622.77	3626.55	3637.35	3641.75	487.88	14.89	4.09
S11	3153.12	3622.04	3625.60	3636.37	3641.73	488.61	15.23	4.46

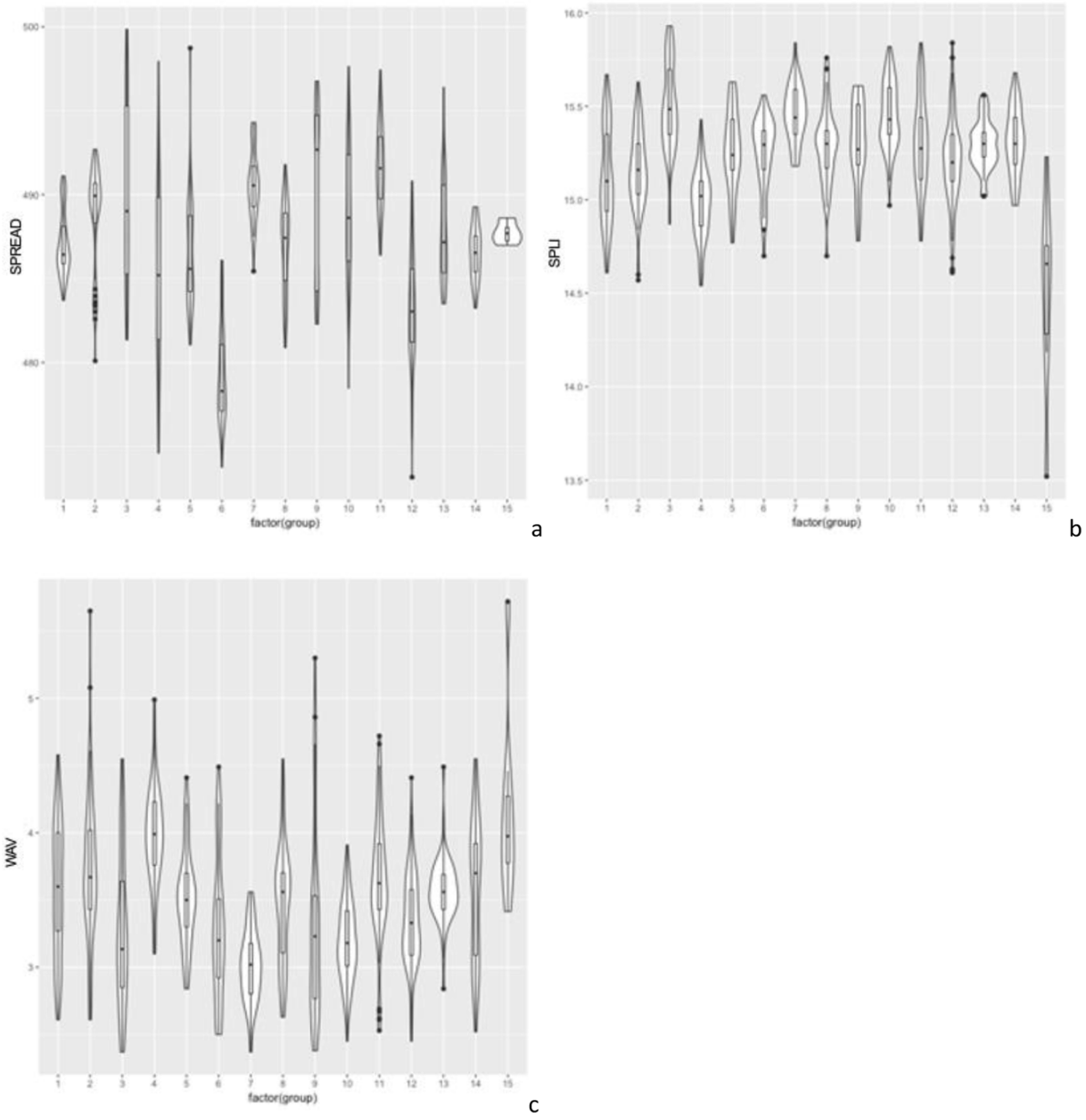

Fig. 5. Violin plots for SPREAD (a), SPLI (b) and WAV (c), respectively. Groups are given by: 1 = Afyon; 2 = Altıntaş; 3 = Aphrodisias; 4 = Carrara; 5 = Denizli; 6 = Ephesus; 7 = Hymettus; 8 = Miletus; 9 = Naxos; 10 = Paros; 11 = Pentelic; 12 = Proconnesus; 13 = Thasos; 14 = Thiountas; 15 = unknown.

steps, thus justifying a clear separation for SPLIT. Notwithstanding this uncertainty, it is also possible to note that the WAV parameter data from the painting presents an evident overlapping with the Carrara group for all the variation range of values and not only for upper or lower ties.

The application of the Kruskal-Wallis test by ranks [33] points out significant differences between some of the 15 groups for all the spectral parameters ($p < 0.05$). The test is a non-parametric method equivalent to the one-way analysis of variance (ANOVA). The subsequent application of the post hoc Kruskal Nemenyi test allowed us to verify, by multiple comparisons between group couples, which groups were more similar/different [31]. Results are reported in Table 2 as p-values (values $\ll 0.05$ indicate significant differences).

Results indicate that group 15, related to the artwork subject of this study, is significantly similar to most of the groups for SPREAD and WAV. Conversely, the SPLIT parameter appears more discriminating, and it reduces the number of affine groups to 4 (groups 1, 2, 4, 12). In comparison with the similarity with all the other groups, a particular closeness with the Carrara group for the WAV and SPLIT parameters is noted (p-value equal to 1 or very near to 1).

By aiming to consider the joint relationships among the variables and verify the homogeneity of the groups constituting the reference database, a cluster analysis was performed on 1061 cases and the three variables, SPLIT, SPREAD, and WAV. The multivariate analysis was performed by using the R Library (R Development Core Team, 2021) for robust analysis (package "cluster") developed following Kaufman and Rousseeuw [25]. Before the analysis, the variables were standardized, and the CLARA algorithm was used. The target was to find 15 natural clusters to be matched with the original 15 geographical groups and verify which geographical group resembles the group of samples extracted from the painting.

Results in Table 3 indicate that the reference database is not homogeneous, as expected. In this context, the painting cases mainly tend to allocate (4 cases) in the natural cluster 2 where the most representative site is the Carrara followed by the Afyon one. The other 4 cases appear to

Table 2
Results of the post hoc Kruskal Nemenyi test (p-values) for SPREAD (a), SPLIT (b), and WAV (c) to point out similarity among the 15 groups.

Pairwise comparisons using Tukey and Kramer (Nemenyi) test
with Tukey-Dist approximation for independent samples

data: SPREAD vs groups

	1	2	3	4	5	6	7	8	9	10	11	12	13	14
2	0.30601	-	-	-	-	-	-	-	-	-	-	-	-	-
3	0.21058	1.00000	-	-	-	-	-	-	-	-	-	-	-	-
4	0.73901	2.6e-05	7.4e-06	-	-	-	-	-	-	-	-	-	-	-
5	0.99997	0.09525	0.06068	0.99994	-	-	-	-	-	-	-	-	-	-
6	1.4e-11	1.7e-13	1.3e-13	4.4e-09	5.2e-07	-	-	-	-	-	-	-	-	-
7	0.00080	0.82773	0.88549	9.4e-10	0.00020	1.4e-13	-	-	-	-	-	-	-	-
8	1.00000	0.25084	0.16903	0.87228	1.00000	1.0e-10	0.00061	-	-	-	-	-	-	-
9	0.35249	1.00000	1.00000	0.00025	0.11848	2.0e-13	0.95796	0.29464	-	-	-	-	-	-
10	0.15333	1.00000	1.00000	1.1e-08	0.04264	3.3e-14	0.46565	0.12037	1.00000	-	-	-	-	-
11	2.2e-08	0.05776	0.08320	1.5e-13	2.0e-08	< 2e-16	0.99976	2.0e-08	0.26031	0.00111	-	-	-	-
12	2.7e-06	1.4e-13	1.1e-13	0.00093	0.01405	0.03161	1.5e-13	1.7e-05	2.9e-12	1.3e-13	< 2e-16	-	-	-
13	0.99706	0.96691	0.92604	0.02768	0.86478	1.3e-13	0.04301	0.99191	0.95880	0.95129	2.1e-05	1.0e-10	-	-
14	0.99999	0.09809	0.06195	0.99975	1.00000	1.7e-07	0.00019	1.00000	0.12365	0.04169	1.3e-08	0.00669	0.88179	-
15	1.00000	0.99996	0.99990	0.99162	0.99993	0.00347	0.88514	1.00000	0.99988	0.99999	0.51270	0.27641	1.00000	0.99996

a

Pairwise comparisons using Tukey and Kramer (Nemenyi) test
with Tukey-Dist approximation for independent samples

data: SPLI vs groups

	1	2	3	4	5	6	7	8	9	10	11	12	13	14
2	1.00000	-	-	-	-	-	-	-	-	-	-	-	-	-
3	6.7e-12	8.5e-10	-	-	-	-	-	-	-	-	-	-	-	-
4	0.00542	0.00107	< 2e-16	-	-	-	-	-	-	-	-	-	-	-
5	0.39067	0.73581	0.00378	3.5e-08	-	-	-	-	-	-	-	-	-	-
6	0.33823	0.70482	0.00098	2.4e-09	1.00000	-	-	-	-	-	-	-	-	-
7	1.1e-09	4.9e-08	1.00000	6.3e-14	0.01228	0.00455	-	-	-	-	-	-	-	-
8	0.03050	0.15827	0.00894	2.9e-13	1.00000	0.99999	0.03079	-	-	-	-	-	-	-
9	0.06449	0.23243	0.06221	1.6e-10	1.00000	0.99998	0.12309	1.00000	-	-	-	-	-	-
10	1.6e-13	5.0e-12	1.00000	< 2e-16	0.00236	0.00036	1.00000	0.00445	0.06257	-	-	-	-	-
11	0.01146	0.08608	0.00395	1.1e-13	1.00000	0.99998	0.01856	1.00000	1.00000	0.00110	-	-	-	-
12	0.88857	0.99725	1.5e-10	4.6e-12	0.98835	0.98649	5.7e-08	0.50795	0.63699	1.4e-13	0.31139	-	-	-
13	0.03393	0.18052	0.00281	1.8e-13	1.00000	1.00000	0.01322	1.00000	1.00000	0.00085	1.00000	0.55873	-	-
14	0.02208	0.10852	0.09176	3.1e-12	0.99988	0.99953	0.17357	1.00000	1.00000	0.09332	1.00000	0.37853	1.00000	-
15	0.32333	0.20759	5.0e-08	0.99886	0.00790	0.00729	1.2e-07	0.00134	0.00161	5.3e-08	0.00094	0.03485	0.00159	0.00083

b

Pairwise comparisons using Tukey and Kramer (Nemenyi) test
with Tukey-Dist approximation for independent samples

data: WAV vs groups

	1	2	3	4	5	6	7	8	9	10	11	12	13	14
2	0.99186	-	-	-	-	-	-	-	-	-	-	-	-	-
3	0.04770	0.00037	-	-	-	-	-	-	-	-	-	-	-	-
4	6.1e-06	0.02099	1.6e-13	-	-	-	-	-	-	-	-	-	-	-
5	1.00000	0.89045	0.53736	1.1e-05	-	-	-	-	-	-	-	-	-	-
6	0.07117	0.00084	1.00000	1.3e-13	0.58263	-	-	-	-	-	-	-	-	-
7	4.6e-08	3.3e-11	0.11523	< 2e-16	4.8e-05	0.17105	-	-	-	-	-	-	-	-
8	0.99832	0.49193	0.65516	3.9e-09	1.00000	0.70459	3.2e-05	-	-	-	-	-	-	-
9	0.09856	0.00183	1.00000	2.5e-13	0.60680	1.00000	0.29721	0.73006	-	-	-	-	-	-
10	1.2e-06	2.0e-10	0.96078	< 2e-16	0.00389	0.98259	0.69067	0.00231	0.99673	-	-	-	-	-
11	0.99918	1.00000	0.00041	0.00074	0.95728	0.00104	1.5e-11	0.62797	0.00249	2.1e-11	-	-	-	-
12	0.04259	0.00011	1.00000	< 2e-16	0.69792	1.00000	0.00255	0.80605	0.99999	0.15016	6.8e-05	-	-	-
13	1.00000	0.99879	0.01761	1.7e-05	0.99992	0.02955	6.8e-09	0.98661	0.04596	9.7e-08	0.99996	0.01156	-	-
14	1.00000	0.99601	0.14018	0.00021	1.00000	0.17564	1.3e-06	0.99965	0.20722	9.1e-05	0.99965	0.18199	1.00000	-
15	0.67445	0.97180	0.01232	1.00000	0.47326	0.01361	1.0e-05	0.29029	0.01427	0.00040	0.92730	0.02026	0.74989	0.69980

c

Table 3
Cross-correlation between the original 15 geographical sites and 15 natural clusters as obtained applying the CLARA algorithm in R.

cluster	1	2	3	4	5	6	7	8	9	10	11	12	13	14	15
Afyon	36	29	0	0	0	0	0	0	0	0	0	0	0	0	0
Altintaş	37	18	1	1	1	0	0	0	0	0	0	0	0	0	0
Aphrodisias	22	7	5	0	0	16	5	4	1	0	0	0	0	0	0
Carrara	36	68	0	1	0	0	6	1	0	32	2	0	0	0	0
Denizli	35	5	0	0	0	0	1	0	0	0	0	0	0	0	0
Ephesus	30	1	11	0	0	0	0	0	0	8	0	0	0	0	0
Hymettus	32	0	0	0	0	9	0	0	0	0	0	1	0	0	0
Miletus	47	10	0	0	0	3	0	0	0	0	0	0	0	0	0
Naxos	23	5	4	0	1	6	1	0	0	0	0	0	0	0	0
Paros	107	2	2	0	0	27	0	4	0	0	0	0	0	0	0
Pentelic	49	13	0	0	0	6	8	2	0	0	0	0	0	0	0
Proconnesos	126	10	6	0	0	2	0	0	0	3	4	1	6	0	0
Thasos	60	7	0	0	0	0	0	2	0	0	0	0	0	0	0
Thiounta	27	15	2	0	0	0	0	0	0	0	0	0	0	0	0
Painting	**0**	**4**	**0**	**0**	**0**	**0**	**0**	**0**	**0**	**0**	**0**	**0**	**1**	**1**	**2**

present an anomalous behavior with no similarity with other geographical locations except a weak affinity for Proconnesus. The fact that some natural clusters occur with no reference to the geographical clusters identified in the original database can be interpreted as an effect of the "noise" of the method. The reduced number of parameters, the small number of samples, and their multilayered structure all concur to add some uncertainty in the discriminating capability of the multivariate analysis. Nevertheless, the multivariate approach provides a clear indication, in complete agreement with what was observed with the Kruskal-Wallis test.

6. Conclusions

The present results provide convincing evidence that the EPR investigation of carbonate materials applied to complex subjects, such as the painting in this study, is a practical approach. On the one hand, the well-known capability of the EPR spectroscopy to selectively focus just on specific ions in the sample allows receiving information despite complex sample phase composition and texture. On the other hand, this procedure enables working with microscopic and lightweight samples, although some cost must be paid in terms of acquisition times and detection limits.

Concerning the original goals of this study, the obtained results allow us to reach the following concluding considerations:

1) The EPR spectra of the carbonate layer in the eight samples, which showed scientifically significant results, are undoubtedly attributed to calcite, thus allowing the identification of the calcium carbonate polymorph as the mineralogical phase applied to the wood panel as a ground preparation layer.
2) The comparison of the EPR spectra of the calcite preparation layer obtained from the painting's samples with those of the chalk revealed some significant differences, which allowed safely excluding that the preparation layer consists of chalk.
3) The geographic origin study was carried out by comparison with an existing database through a specifically designed statistical analysis of the spectral parameters. Although some significant limitations were induced by this method (sample mass, number of EPR parameters, poor variability), the geographic origin study was still feasible and scientifically valid. It provided apparent similarity between the group of the painting samples and some groups in the database, including the Carrara group.

The conclusions reached of the present study provide valuable suggestions to the investigation of the painting's history in its general context. In particular, the highly likely pertinence of the preparation layer's calcite to marble from the Apuan Alps (Carrara) could favor the possible Italian origin of the painting; moreover, it can potentially offer further compatibility clues in the process of the painting's attribution. However, the future identification of additional variables to be implemented in the used protocol can further improve and narrow down the assessment of the geographical provenance by taking into account the variability of these types of matrices.

CRediT authorship contribution statement

Maurizio Romanelli: Conceptualization, Methodology, Investigation, Writing – original draft, Writing – review & editing. **Antonella Buccianti:** Conceptualization, Methodology, Formal analysis, Writing – original draft, Writing – review & editing. **Francesco Di Benedetto:** Conceptualization, Methodology, Investigation, Writing – original draft, Writing – review & editing. **Lorenzo Bellucci:** Investigation, Resources, Writing – original draft, Writing – review & editing. **Stefan Cemicky:** Resources, Writing – original draft, Writing – review & editing.

Declaration of Competing Interest

The authors declare that they have no known competing financial interests or personal relationships that could have appeared to influence the work reported in this paper.

Acknowledgements

This research was funded under the Progetto di Ateneo (Università degli Studi di Firenze) programme to MR, AB and FDB and by DRIART AG. FDB also acknowledges FAR2021 funds of the Università degli Studi di Ferrara.

Appendix A. Supplementary data

Supplementary data to this article can be found online at https://doi.org/10.1016/j.microc.2022.107219.

References

[1] K. Al-Bashaireh, A.Q. Al-Housan, Provenance investigation of white marbles of chancel screens from Rihab Byzantine churches, northeast Jordan, J. Cult. Herit. 16 (4) (2015) 591–596.
[2] J.G. Angus, J.B. Raynor, M. Robson, Reliability of experimental partition coefficients in carbonate systems: evidence for inhomogeneous distribution of impurity cations, Chem. Geol. 27 (3) (1979) 181–205.
[3] G. Armiento, D. Attanasio, R. Platania, Electron spin resonance characterization and provenance of marbles: the case of the "Cipollino Verde", MRS Online Proc. Library 462 (1996) 331–336.
[4] G. Armiento, D. Attanasio, R. Platania, Electron spin resonance study of white marbles from Tharros (Sardinia): a reappraisal of the technique, possibilities and limitations, Archaeometry 39 (2) (1997) 309–319.
[5] D. Attanasio, The use of electron spin resonance spectroscopy for determining the provenance of classical marbles, Appl. Magn. Reson. 16 (3) (1999) 383–402.

[6] D. Attanasio, Ancient White Marbles. Identification and analysis by Paramagnetic Resonance Spectroscopy. Studia Archaeologica, 122, L'Erma di Bretschneider, Roma, 2003, 284p.
[7] D. Attanasio, G. Armiento, M. Brilli, M.C. Emanuele, R. Platania, B. Turi, Multimethod marble provenance determinations: the Carrara marbles as a case study for the combined use of isotopic, electron spin resonance and petrographic data, Archaeometry 42 (2) (2000) 257–272.
[8] D. Attanasio, C. Boschi, S. Bracci, E. Cantisani, F. Paolucci, The Greek and Asiatic marbles of the Florentine Niobids, J. Archaeol. Sci. 66 (2016) 103–111.
[9] D. Attanasio, M. Brilli, M. Bruno, The properties and identification of marble from Proconnesos (Marmara Island, Turkey): a new database including isotopic, EPR and petrographic data, Archaeometry 50 (5) (2008) 747–774.
[10] D. Attanasio, M. Brilli, N. Ogle, The Isotopic Signature of Classical Marbles. Studia Archaeologica, 145, L'Erma di Bretschneider, Roma, 2006, 336p.
[11] D. Attanasio, M. Bruno, W. Prochaska, A.B. Yavuz, Ancient 'black' decorative stones and the Ephesian origin of sculptural Bigio antico, Archaeometry 59 (5) (2017) 794–814.
[12] D. Attanasio, R. Platania, P. Rocchi, The marble of the David of Michelangelo: a multi-method analysis of provenance, J. Archaeol. Sci. 32 (2005) 1369–1377.
[13] V. Baïetto, G. Villeneuve, M. Schvoerer, F. Bechtel, N. Herz, Investigation of electron paramagnetic resonance peaks in some powdered Greek white marbles, Archaeometry 41 (2) (1999) 253–265.
[14] G.E. Barberis, R. Calvo, H.G. Maldonado, C.E. Zarate, EPR spectra and linewidths of Mn^{2+} in calcite, Phys. Rev. B 12 (1975) 853–860.
[15] B. Bleaney, R.S. Rubins, Explanation of some 'Forbidden' Transitions in Paramagnetic Resonance, Proc. Phys. Soc. (London) 77 (1961) 103–112.
[16] M. Brilli, L. Conti, F. Giustini, M. Occhiuzzi, P. Pensabene, M. De Nuccio, Determining the provenance of black limestone artefacts using petrography, isotopes and EPR techniques: the case of the monument of Bocco, J. Archaeol. Sci. 38 (6) (2011) 1377–1384.
[17] M. Brilli, M.P. Lapuente Mercadal, F. Giustini, H. Royo, Plumed Petrography and mineralogy of the white marble and black stone of Göktepe (Muğla, Turkey) used in antiquity: New data for provenance determination, J. Archaeol. Sci.: Reports 19 (2018) 625–642.
[18] D. Covaci, O.G. Duliu, Preliminary EPR spectra database of natural carbonate of some Romanian quarries, Rom. Rep. Phys. 65 (2) (2013) 487–494.
[19] D. Covaci, D. Seletchi, O.G. Duliu, EPR study on Mn^{2+} homogeneity in travertine deposits from Borsec Quarry, Rom. Rep. Phys. 64 (3) (2012) 761–767.
[20] N.P. Crook, S.R. Hoon, K.G. Taylor, C.T. Perry, Electron spin resonance as a high sensitivity technique for environmental magnetism: determination of contamination in carbonate sediments, Geophys. J. Int. 149 (2) (2002) 328–337.
[21] F. Di Benedetto, A. Buccianti, G. Montegrossi, M. Innocenti, C.A. Massa, L.A. Pardi, M. Romanelli, EPR discrimination of microcrystalline calcite geomaterials, Am. Miner. 97 (2012) 1619–1626.
[22] O.G. Duliu, M. Velter-Stefanescu, Numerical taxonomy: Mn^{2+} EPR line shape as a criterion in provenance studies, J. Optoelectron. Adv. Mater. 8 (4) (2006) 1557–1561.
[23] O.G. Duliu, M.N. Grecu, C. Cristea, EPR and X-Ray Diffraction investigation of some greek marbles and limestones, Rom. Rep. Phys. 61 (3) (2009) 487–499.
[24] J.L. Hintze, R.D. Nelson, Violin plots: a box plot-density trace synergism, Am. Stat. 52 (2) (1998) 181–184, 10.1080%2F00031305.1998.10480559.
[25] L. Kaufman, P.J. Rousseeuw, Finding groups in data: An introduction to cluster analysis, Wiley-Intersci.: New York (Series in Applied Probability and Statistics) (1990).
[26] D. Kralj, J. Kontrec, L. Brecœvic, G. Falini, V. Nothig-Laslo, Effect of inorganic anions on the morphology and structure of magnesium calcite, Chem. Eur. J. 10 (2004) 1647–1656.
[27] Y. Maniatis, D. Tambakopoulos, E. Dotsika, T. Stefanidou-Tiveriou, Marble provenance investigation of Roman sarcophagi from Thessaloniki, Archaeometry 52 (1) (2010) 45–58.
[28] J. Pijoan, Summa Artis. Historia General del Arte. Vol. XIV, Renacimiento Romano y Veneciano, Siglo XVI, Espasa-Calpe, s.a, Madrid, 1961.
[29] S. Piligkos, I. Laursen, A. Morgenstjerne, H. Weihe, Sign and magnitude of Spin Hamiltonian parameters for Mn^{2+} impurities in calcite. A multi- and low-frequency EPR study, Mol. Phys. 115 (2007) 2025–2050.
[30] K. Polikreti, Y. Maniatis, A new methodology for the provenance of marble based on EPR spectroscopy, Archaeometry 44 (1) (2002) 1–21.
[31] R Development Core team, R: a language and environment for statistical computing. R Foundation for Statistical Computing, Vienna, Austria, http://www.R-project.org. Accessed the November, 4th, 2021.
[32] R.A. Shepherd, W.R.M. Graham, EPR of Mn^{2+} in polycrystalline dolomite, J. Chem. Phys. 81 (1984) 6080–6084.
[33] J.D. Spurrier, On the null distribution of the Kruskas-Wallis H statistics, J. Nonparam. Stat. 15 (6) (2003) 685–691.
[34] M.J.N. Stols-Witlox, Grounds, 1400–1900, in: J.H. Stoner, R. Rushfield (Eds.), The Conservation of Easel Paintings, Routledge, London, 2012, pp. 161–185.
[35] M.J.N. Stols-Witlox, Historical recipes for preparatory layers for oil paintings in manuals, manuscripts and handbooks in North West Europe, 1550–1900: analysis and reconstructions, University of Amsterdam, 2014.
[36] D. Tambakopoulos, T. Stefanidou-Tiveriou, E. Papagianni, Y. Maniatis, Provenance investigation of Roman marble sarcophagi from Nicopolis, Epirus, Greece: revealing a strong artistic and trade connection with Athens, Archaeol. Anthropol. Sci. 11 (2) (2019) 597–608.
[37] M.C. Thrun, T. Gehlert, A. Ultsch, F. Vafaee, Analyzing the fine structure of distributions, PLoS ONE 15 (10) (2020) e0238835.
[38] A.B. Vassilikou-Dova, EPR-determined site distributions of low concentrations of transition-metal ions in minerals: review and predictions, Am. Miner. 78 (1–2) (1993) 49–55.
[39] H. Weihe, S. Piligkos, A.L. Barra, I. Laursen, O. Johnsen, EPR of Mn^{2+} impurities in calcite: a detailed study pertinent to marble provenance determination, Archaeometry 51 (1) (2009) 43–48.
[40] T.R. Wildeman, The distribution of Mn^{2+} in some carbonates by electron paramagnetic resonance, Chem. Geol. 5 (3) (1970) 167–177.
[41] A.B. Yavuz, M. Bruno, D. Attanasio, An updated, multi-method database of Ephesos marbles including white, greco scritto and bigio varieties, Archaeometry 53 (2) (2011) 215–240.